Structure, Spectra and Redox Behaviour of Copper(II) Complexes of Bis(benzimidazolyl)diamine Ligands†

Thangarasu Pandiyan,[a] **Mallayan Palaniandavar,**[*,a] **M. Lakshminarayanan**[b] **and Hattikudur Manohar**[b]
[a] *Department of Chemistry, Bharthidasan University, Tiruchirapalli-620 024, Tamil Nadu, India*
[b] *Inorganic and Physical Chemistry Department, Indian Institute of Science, Bangalore-560 012, India*

The linear quadridentate ligand *N,N'*-bis(benzimidazol-2-ylethyl)ethane-1,2-diamine (L^1) and its 1-methylbenzimidazole analogue (L^2) and homologues form 1 : 1 complexes with $Cu(ClO_4)_2$; L^1 also forms complexes of the types CuL^1X_2 where X = NO_3, PF_6, Br or Cl and $CuL^1(X)Y$ where X = Cl or Br and Y = ClO_4 or Br. Deep blue $CuL^1Br_2{\cdot}2H_2O$ crystallizes in the monoclinic space group $C2/c$ with $Z = 4$, $a = 9.919(2)$, $b = 16.626(3)$, $c = 14.102(3)$ Å and $\beta = 94.39(2)°$. The structure was solved by Patterson and Fourier difference methods and refined by the least-squares technique to $R = 0.064$ for 2195 independent reflections with $I > 1.5\sigma(I)$. The molecule lies on a two-fold axis symmetrically around Cu^{II}. The co-ordination around Cu^{II} is found to be square planar with two amino nitrogens and two benzimidazole nitrogens forming the equatorial plane [Cu–N 1.983(3) and 2.037(4) Å]. The bromides are at longer distances [3.349(1) Å] in axial sites. Ligand field and EPR spectra indicate that one bromide or chloride ion is axially co-ordinated to Cu^{II} in $[CuL^1]^{2+}$. This ion exhibits quasi-reversible redox behaviour. Electrochemical studies of the dihalides in methanol have established the presence of $[CuL^1X_2]$, $[CuL^1(X)]^+$ and $[CuL^1]^{2+}$ in equilibrium. In complexes with 565 $[CuL^4]^{2+}$ [L^4 = *N,N'*-bis(benzimidazol-2-ylmethyl)ethane-1,2-diamine] and 555 $[CuL^3]^{2+}$ [L^3 = *N,N'*-bis(1-methylbenzimidazol-2-ylmethyl)propane-1,3-diamine] chelate rings, Cu^{II} does not seem to lie in the N_4 square plane, as revealed by their low $A_{\parallel}$ values and irreversible electrochemical behaviour. The Cu^{II}–Cu^{I} redox potentials in methanol are in the order $[CuL^1]^{2+} < [CuL^3]^{2+} < [CuL^4]^{2+}$; this illustrates that six-membered chelate rings are suitable to stabilize Cu^{II}, when Cu–N σ interactions are favourable.

Histidine (imidazole) ligands are known to constitute the active site of numerous copper proteins such as plastocyanin,[1] azurin[2] and deoxyhaemocyanin.[3] As synthetic analogues of the active sites of various metalloproteins have been useful in elucidating the relation between their structure, electronic properties and functions, copper complexes of imidazole ligands are of interest as models for copper proteins. However, surprisingly, only a few such copper complexes[4,5] have been characterized, obviously because of the synthetic difficulties involving the imidazole moiety. So the synthetically accessible benzimidazoles have recently become potential ligands[6–9] for constructing models for copper proteins. Further, the bulkiness of the benzimidazole moiety may impose around copper(II) unusual geometries which are responsible for the unique properties of the proteins. Nishida and Takahashi[10] have determined the crystal structure of several 1:1 copper(II) complexes of bis(benzimidazole-2-ylmethyl)amine and its homologues with alkyl substituents on the amine nitrogen atom, to elucidate the unusual changes in $A_{\parallel}$ values. Palaniandavar and co-workers[11] have determined the X-ray crystal structure, spectra and redox behaviour of 1:2 complexes of this ligand.

The present contribution aims at incorporating one more NH group in this tridentate ligand and elucidating the effect of bulky benzimidazole, varying chelate ring size and methyl substitution on the benzimidazole ring and/or chelate backbone in copper(II) complexes of bis(benzimidazol-2-yl)diamines L^1–L^7 on the structure, spectra and redox behaviour.

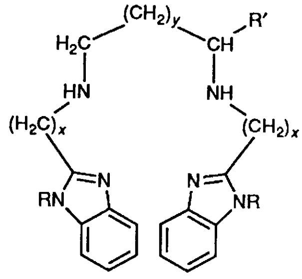

	x	y	R	R'
L^1	2	0	H	H
L^2	2	0	Me	H
L^3	1	1	Me	H
L^4	1	0	H	H
L^5	1	0	Me	H
L^6	1	0	H	Me
L^7	1	0	Me	Me

Experimental

Materials.—Reagents were used as received from G. F. Smith $[Cu(ClO_4)_2{\cdot}6H_2O]$, BDH, India $[Cu(NO_3)_2{\cdot}3H_2O$, $CuCl_2{\cdot}2H_2O$, $CuBr_2]$, SISCO, India (1,2-diaminobenzene), Kodak (*N*-methyl-1,2-diaminobenzene dihydrochloride), E. Merck, India (ethane-1,2-diamine, 1,2-diaminopropane and 1,3-diaminopropane) and Aldrich (2-chloromethylbenzimidazole). Tetra-*n*-hexylammonium perchlorate (G. F. Smith) was recrystallized twice from aqueous ethanol.

Synthesis of Ligands.—*N,N'*-Bis(benzimidazol-2-ylethyl)ethane-1,2-diamine (L^1) and *N,N'*-bis(1-methylbenzimidazol-2-ylethyl)ethane-1,2-diamine (L^2) were synthesised as reported elsewhere.[12]

2-*Chloromethyl*-1-*methylbenzimidazole hydrochloride*. Gly-

---

† *Supplementary data available:* see Instructions for Authors, *J. Chem. Soc., Dalton Trans.*, 1992, Issue 1, pp. xx–xxv.

Table 1 Elemental analyses of the copper(II) complexes with calculated values in parentheses

	Analysis (%)			
Compound	C	H	N	Cu
$CuL^1(ClO_4)_2$	39.30	3.95	13.55	10.25
	(39.30)	(3.95)	(13.75)	(10.40)
$CuL^1Cl_2{\cdot}2H_2O$	46.00	5.25	15.95	12.45
	(46.30)	(5.45)	(16.20)	(12.25)
$CuL^1Br_2{\cdot}2H_2O$	39.20	4.65	13.80	10.15
	(39.50)	(4.65)	(13.85)	(10.45)
$CuL^1(NO_3)_2$	44.90	4.50	20.70	11.65
	(44.80)	(4.50)	(20.90)	(11.85)
$CuL^1(PF_6)_2{\cdot}H_2O$	33.55	3.45	11.50	8.70
	(33.35)	(3.65)	(11.65)	(8.85)
$CuL^1Cl(Br){\cdot}H_2O$	44.30	4.65	15.20	11.45
	(44.05)	(4.80)	(15.40)	(11.65)
$CuL^1Br(ClO_4){\cdot}H_2O$	39.35	4.20	13.70	10.10
	(39.40)	(4.30)	(13.80)	(10.45)
$CuL^2(ClO_4)_2$	41.15	4.40	13.00	9.95
	(41.35)	(4.40)	(13.15)	(9.95)
$CuL^3(ClO_4)_2$	40.00	4.00	13.10	10.00
	(40.35)	(4.20)	(13.45)	(10.15)
$CuL^4(ClO_4)_2$	37.20	3.45	14.30	10.85
	(37.00)	(3.45)	(14.40)	(10.90)
$CuL^5(ClO_4)_2{\cdot}H_2O$	38.40	3.95	13.05	10.95
	(38.20)	(4.15)	(13.35)	(10.10)
$CuL^6(ClO_4)_2$	38.55	3.65	13.95	10.45
	(38.25)	(3.70)	(14.10)	(10.65)
$CuL^7(ClO_4)_2{\cdot}2H_2O$	38.50	4.75	12.50	9.55
	(38.15)	(4.55)	(12.70)	(9.60)

colic acid (0.1 mol) was refluxed (24 h) with *N*-methyl-1,2-diaminobenzene dihydrochloride (0.1 mol) in 6 mol dm^{-3} HCl (200 cm^3). The hydrochloride obtained was filtered off and washed with ethanol, then suspended in water and neutralized with aqueous ammonia. The precipitate obtained was filtered off, washed with water and dried in vacuum. The product (0.05 mol) was suspended in dichloromethane (50 cm^3) and thionyl chloride (10 cm^3) was added slowly (1 h). The reaction mixture was refluxed on a water-bath then cooled. The unreacted thionyl chloride was removed by adding a small amount of methanol. The hydrochloride formed was collected and dried over $CaCl_2$ in vacuum (Found: C, 49.75; H, 4.60; N, 12.80. Calc. for $C_9H_{10}Cl_2N_2$: C, 49.80; H, 4.70; N, 12.90%).

L^3–L^7. These were synthesised by the condensation of 2-chloromethylbenzimidazole or 2-chloro-1-methylbenzimidazole dihydrochloride with the corresponding diamine using NaOMe as base. A typical procedure for the synthesis of L^4 is given below. Ethane-1,2-diamine (0.001 mol) in methanol (20 cm^3) was added slowly to a solution of 2-chloromethylbenzimidazole (0.002 mol) in methanol (20 cm^3). To this solution was added with stirring a solution of sodium methoxide (0.002 mol) over a period of 2 h and the resulting solution was refluxed for 0.5 h. It was then filtered, passed through an acidic alumina column and used for the preparation of the copper complexes.

Synthesis of Complexes.—$CuL^1(ClO_4)_2$. The ligand L^1 (1 mmol) was dissolved in methanol (10 cm^3) and to this was added with stirring a solution of $Cu(ClO_4)_2{\cdot}6H_2O$ (1 mmol) in methanol (5 cm^3). The blue complex obtained was collected and dried over P_4O_{10}. This procedure was also employed to obtain $CuL^2(ClO_4)_2$. Using the above procedure the perchlorates of L^3–L^7 were prepared by treating the methanol solution of the ligands prepared above with an equimolar amount of $Cu(ClO_4)_2{\cdot}6H_2O$ in methanol. All the complexes were obtained in high yields and their analytical data are collected in Table 1.

$CuL^1X_2{\cdot}nH_2O$ (X = Cl, Br or NO_3). A solution of L^1 in methanol was mixed with an equimolar quantity of the corresponding copper salt in methanol and the coloured complex formed was collected and dried over P_4O_{10}.

A solution of the above bromide complex (0.01 g) in methanol (10 cm^3) was allowed slowly to evaporate. The fine blue single crystals obtained were suitable for X-ray diffraction.

$CuL^1(PF_6)_2{\cdot}H_2O$. To L^1 (1 mmol) dissolved in methanol (20 cm^3) was added a solution of $CuCl_2{\cdot}2H_2O$ (1 mmol) in methanol (20 cm^3). Addition of a saturated aqueous solution (3 cm^3) of KPF_6 followed by reduction in volume led to the formation of blue crystals. These were collected and dried over P_4O_{10} in vacuum.

$CuL^1Cl(Br){\cdot}H_2O$. The ligand L^1 (0.5 mmol) was dissolved in methanol (20 cm^3) and to this was added a solution of $CuCl_2{\cdot}2H_2O$ (0.25 mmol) and $CuBr_2$ (0.25 mmol) in methanol (20 cm^3). The blue solution was allowed to stand at room temperature. The fine blue crystals formed were collected and dried over P_4O_{10} in vacuum.

$CuL^1Br(ClO_4){\cdot}H_2O$. The ligand L^1 (0.5 mmol) was dissolved in methanol (20 cm^3) and to this was added a solution of $CuBr_2$ (0.25 mmol) and $Cu(ClO_4)_2{\cdot}6H_2O$ (0.25 mmol) in methanol (10 cm^3). The blue complex formed was separated and dried over P_4O_{10} in vacuum.

Physical Measurements.—Elemental analyses were performed at City University, London. The copper content was determined by atomic absorption. Diffuse reflectance and solution spectra in methanol and acetonitrile were measured on a Hitachi U-3400 double-beam UV/VIS/NIR spectrophotometer, EPR spectra on a Varian E-12 X-band spectrometer calibrated with diphenylpicrylhydrazyl (dpph). The values of g_0 and A_0 were measured at ambient temperature and $g_\parallel$, $A_\parallel$ and $g_\perp$ at 77 K. Second-order corrections[13] were applied to the resonance field of the transitions from which g_0 and A_0 were obtained.

Cyclic voltammetry and differential pulse voltammetry at a platinum-sphere electrode were performed at 25 ± 0.2 °C. The temperature of the electrochemical cell was maintained by a cryocirculator (Hakke D8 G). The solutions were deoxygenated by bubbling of research-grade nitrogen. The instrument utilized included a EG & G PAR 273 potentiostat. An IBM PS-2 computer with EG & G M270 software was employed to carry out the experiments and to acquire the data. A HP plotter (DMP 40) was used to plot the cyclic voltammograms. A three-electrode cell configuration was employed, the reference electrode being Ag(s)–$AgNO_3$ (0.01 mol dm^{-3}), $N(C_6H_{13})_4ClO_4$ (0.1 mol dm^{-3}) in acetonitrile. Methanol for electrochemistry was distilled over magnesium turnings and acetonitrile over P_4O_{10}.

Crystallographic Data Collection and Structure Analysis of $CuL^1Br_2{\cdot}2H_2O$.—Preliminary cell parameters, obtained from rotation and Weissenberg photographs, were refined by a least-squares procedure applied to 25 carefully centred reflections on a CAD4 single-crystal diffractometer. Details of the data collection and processing are in Table 2. The data were corrected for Lorentz, polarization and absorption effects.[14]

The structure was solved by conventional Patterson and Fourier methods. All the hydrogen atoms, except those belonging to the lattice water, were located from difference electron-density maps, but their positions were not refined. Their *U* values were fixed at 0.05 Å.[15] The final difference electron-density map revealed no peaks higher than 0.76 e Å^{-3} at *ca.* 1.0 Å from the copper and bromine positions.

The SHELX 76 system of programs[15] was used for structure analysis and refinement and a DEC 1090 computer for calculations. Diagrams were drawn using the ORTEP II[16] and PLUTO 78[17] programs. The scattering factors for H, C, O, N and Br were used as available[17] in the SHELX 76 program and for Cu they were taken from ref. 18 (anomalous dispersion corrections applied). The final atomic coordinates are given in Table 3.

Additional material available from the Cambridge Crystallo-

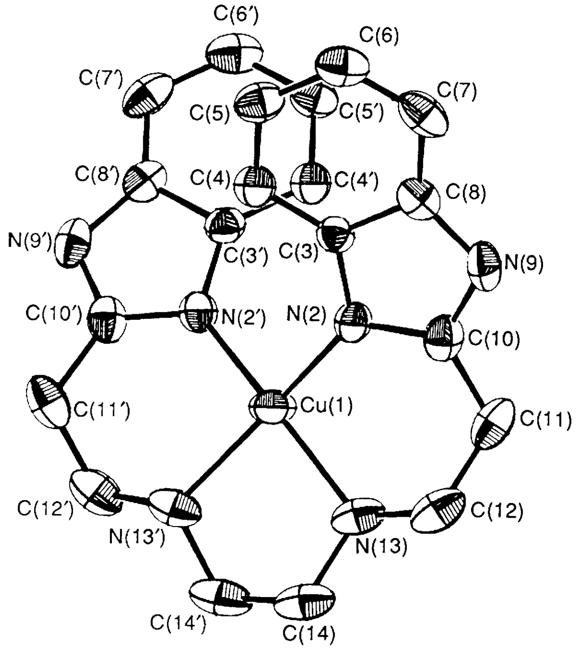

Fig. 1 An ORTEP drawing of the $[CuL^1]^{2+}$ cation showing the atom numbering and the thermal motion ellipsoids (50% probability level) for non-hydrogen atoms

Table 2 Crystal data for $CuL^1Br_2{\cdot}2H_2O$

Formula	$C_{20}H_{28}Br_2CuN_4O_2$
M	607.83
Crystal symmetry	Monoclinic
Space group	$C2/c$
a/Å	9.919(2)
b/Å	16.626(3)
c/Å	14.102(3)
β/°	94.39(2)
U/Å^3	2318.78
Z	4
μ/cm^{-1}	46.6 cm^{-1}
Crystal dimensions/mm	0.18 × 0.32 × 0.55
F(000)	1180.00
D_c/g cm^{-3}	1.741
D_m^{a}/g cm^{-3}	1.75
λ(Mo-Kα)/Å	0.710 69
T/K	294
Scan type	ω–2θ
θ range/°	2.5–28.5
No. of reflections measured	3640
No. of observed reflections [$F_o > 3\sigma(F_o)$]	2195
Weighting scheme	$k[\sigma^2(F_o) + gF_o^2]^{-1}$
R^b	0.064
R'^c	0.059

^{a} By flotation in $CHCl_3 + CHBr_3$. ^{b} $\Sigma(|F_o| - |F_c|)/\Sigma|F_o|$. ^{c} $[\Sigma w(|F_o| - |F_c|)^2/\Sigma|F_o|^2]^{\frac{1}{2}}$.

Table 3 Fractional atomic coordinates (× 10^5 for Cu and Br, × 10^4 for the rest) with their estimated standard deviations (e.s.d.s) in parentheses

Atom	x	y	z
Cu(1)	0	10 747(0)	25 000
N(2)	1 291(3)	1 844(2)	3 147(2)
C(3)	1 064(4)	2 596(2)	3 558(3)
C(4)	−124(4)	2 990(3)	3 724(3)
C(5)	−11(5)	3 740(3)	4 158(3)
C(6)	1 242(5)	4 092(3)	4 398(3)
C(7)	2 432(5)	3 695(3)	4 270(3)
C(8)	2 323(4)	2 943(3)	3 855(3)
N(9)	3 276(3)	2 384(2)	3 623(3)
C(10)	2 636(4)	1 747(3)	3 219(3)
C(11)	3 354(5)	1 022(3)	2 920(3)
C(12)	2 657(5)	249(3)	3 139(3)
N(13)	1 364(4)	157(2)	2 567(3)
C(14)	678(6)	−606(3)	2 773(3)
Br(1)	15 161(5)	10 253(3)	4 586(3)
O(1)	3 850(3)	2 495(2)	1 101(2)

Table 4 Bond lengths (Å) involving non-hydrogen atoms with e.s.d.s in parentheses

Cu(1)–N(2)	1.983(3)	C(7)–C(8)	1.381(7)
Cu(1)–N(13)	2.037(4)	C(8)–N(9)	1.383(6)
N(2)–C(3)	1.403(5)	N(9)–C(10)	1.338(6)
N(2)–C(10)	1.340(5)	C(10)–C(11)	1.479(7)
C(3)–C(4)	1.384(6)	C(11)–C(12)	1.502(7)
C(3)–C(8)	1.410(6)	C(12)–N(13)	1.470(6)
C(4)–C(5)	1.389(7)	N(13)–C(14)	1.478(6)
C(5)–C(6)	1.391(7)	C(14)–C(14′)	1.497(8)
C(6)–C(7)	1.376(7)		

Table 5 Bond angles (°) involving non-hydrogen atoms with e.s.d.s in parentheses

N(2)–Cu(1)–N(2′)	99.6(1)	C(6)–C(7)–C(8)	116.7(4)
N(2)–Cu(1)–N(13)	93.4(1)	C(3)–C(8)–C(7)	122.3(4)
N(2)–Cu(1)–N(13′)	155.3(1)	C(3)–C(8)–N(9)	105.1(4)
C(5)–C(6)–C(7)	121.7(4)	C(8)–N(9)–C(10)	108.8(4)
N(13)–Cu(1)–N(13′)	82.9(2)	N(2)–C(10)–N(9)	112.0(4)
C(4)–C(5)–C(6)	121.6(4)	N(2)–C(10)–C(11)	125.1(4)
Cu(1)–N(2)–C(10)	124.2(3)	N(13)–C(14)–C(14′)	107.9(4)
C(3)–N(2)–C(10)	105.4(3)	C(10)–C(11)–C(12)	113.6(4)
C(3)–C(4)–C(5)	117.3(4)	C(11)–C(12)–N(13)	111.9(4)
N(2)–C(3)–C(8)	108.7(3)	Cu(1)–N(13)–C(12)	119.7(3)
C(4)–C(3)–C(8)	120.1(4)	Cu(1)–N(13)–C(14)	109.7(3)

graphic Data Centre comprises H-atom coordinates, thermal parameters and remaining bond lengths and angles.

Results and Discussion

Description of the Structure of $CuL^1Br_2{\cdot}2H_2O$ *and Comparison with Related Structures.*—An ORTEP diagram of the cation $[CuL^1]^{2+}$ is shown in Fig. 1. Selected bond distances and angles are presented in Tables 4 and 5 respectively. The molecule $[CuL^1]^{2+}$ lies on a two-fold axis of symmetry. The Cu^{II} has a square-planar co-ordination involving two nitrogens of the ethanediamine group and two nitrogens from two benzimidazole groups. The N atoms show small but significant tetrahedral distortions (±0.37 and ±0.43 Å) from the equatorial plane. The $Cu{-}N_{amine}$ and $Cu{-}N_{bzim}$ distances, 2.037(4) and 1.983(3) Å respectively, are in the range of values found in similar compounds.[6–8,19,20] There are two bromide ions at much longer distances of 3.349(1) Å at approximately axial positions, the Cu···Br vector making an angle of 8.4° with the normal to the basal plane. These can at best be considered as weak bonding interactions, in comparison with the co-ordinating distance of 2.417(3) Å observed in $[CuL^8(Br)]^+$ [L^8 = 1,6-bis(benzimidazol-2-yl)-2,5-dithiahexane] ion.[21] The dimensions of the benzimidazole and ethanediamine moieties are normal. The dihedral angle between the two benzimidazole groups is 50.5°. The copper is 0.20 Å out of the plane of the benzimidazole ring. Torsion angles and mean plane calculations indicate that both the five- and six-membered chelate rings assume half-chair conformations.[22]

In the lattice the $[CuL^1]^{2+}$ cations lie in sheets approximately in the (001) plane with Br^- ions and lattice waters in between. The structure is stabilized through hydrogen bonds and van der Waals interactions. The atoms N(13) of ethanediamine and N(9) of benzimidazole, O(1) of the lattice water and Br^- are involved in a network of hydrogen bonds (Table 6).

Table 6 Possible hydrogen bonds

D–H $\cdots$ A	D–H/Å	D $\cdots$ A/Å	H $\cdots$ A/Å	D–H $\cdots$ A/°
N(13)–H(13) $\cdots$ Br(1)	0.96	3.319	2.67	125.9
N(9)–H(9) $\cdots$ O^{I}	0.90	2.854	1.96	168.0
O(1) $\cdots$ Br(1)	—	3.439	—	—
O(1) $\cdots$ $Br(1)^{II}$	—	3.302	—	—

Symmetry codes: I $1 - x, y, \frac{1}{2} - z$; II $\frac{1}{2} - x, \frac{1}{2} - y, -z$.

Short contacts (< 3.7 Å) are given in the Supplementary data. The hydrogen bonding of Br^- to lattice water rather than steric hindrance from the aromatic rings may account for the long Cu $\cdots$ Br bond.

While the present work was in progress our attention was drawn to the structure of a copper(II) complex with the same ligand, but with ClO_4^- as counter ion.[23,*] The complex is a clear cation distortion isomer[24] of the present bromide complex. The tetrahedral distortion (ω)[25] in the bromide (32.5°) is slightly smaller than that (38.8°) in the perchlorate.

A very low trigonality ($\tau = 0.15$)[8] for $CuL^1(ClO_4)_2$ and no trigonality for CuL^1Br_2 indicate that six-membered chelate ring systems, because of the unstrained chair conformation, lead to a very low steric constraint at copper(II). However, the limited bite exhibited by the five-membered chelate ring with a half-chair conformation and the bulky benzimidazole enhance the steric constraint at copper and induce distortion in the N_4 plane. Though the decrease in chelate ring size in the order $[CuL^1]^{2+}$, $[CuL^3]^{2+}$ and $[CuL^4]^{2+}$ would lead to increased trigonality, the strong Cu–NH σ bonds favour planarity. So it is not unreasonable to expect $[CuL^4]^{2+}$, and to a lesser extent $[CuL^3]^{2+}$, to adopt a distorted square-planar structure with Cu^{II} pushed out of the square plane and co-ordinated to ClO_4^- as the fifth ligand, as in the CuN_4 system[26] [Cu(trien)(SCN)]SCN (trien = triethylenetetraamine). Also in the crystal structure[21,27] of $[CuL^9][ClO_4]_2$ [L^9 = 1,2-bis(2,2′-bipyridin-6-yl)ethane] with a 565 chelate ring system a tetrahedral distortion of 35° is observed. Unfortunately, attempts to obtain single crystals of $CuL^3(ClO_4)_2$ and $CuL^4(ClO_4)_2$ to establish a structural correlation based on τ and also to determine how the chelate ring sizes determine the variation of stereochemistry due to the plasticity effect were in vain.

Electronic Absorption Spectra.—All of the complexes, except the chloride and bromides, display a single broad absorption band in the range 15 300–16 900 cm^{-1} (Table 7). Square-planar complexes with CuN_4 chromophores[28–30] usually have band maxima in the range 17 000–19 000 cm^{-1}. The lower values observed may be due to either axial[31] interaction by anions and/or distortion from planarity. All the solid-state (reflectance) spectra are much broader than the solution spectra and seem to contain at least two transitions, showing that the complexes tend to assume square-pyramidal geometry, with Cu^{II} apically co-ordinating to ClO_4^- as revealed in the X-ray crystal structure[23] of $CuL^1(ClO_4)_2$. It has been shown[32] that such a geometry may lead to two well separated transitions.

On dissolution in methanol, however, only one relatively sharp band is observed; this suggests structural changes such as dissociation of co-ordinated ClO_4^- or axial solvent. Addition of an excess of ClO_4^- as $N(C_6H_{13})_4ClO_4$ to $CuL^1(ClO_4)_2$ in methanol does not cause any appreciable change in the spectra. However, for some compounds like $CuL^1(ClO_4)_2$ the band position in acetonitrile is slightly blue-shifted on addition of excess of $NaClO_4$, indicating dissociation of ClO_4^-.

The position of the visible band, for the simple and mixed halides, both in the solid state and in solution, is distinctly lower than that of the perchlorate, indicating that halide ion is co-ordinated to Cu^{II} axially.[31] Further, addition of Br^- or Cl^- as tetrabutylammonium salts to $CuL^1(ClO_4)_2$ in methanol gradually shifted the visible band to lower energy with increase or decrease in ε.

Among the 555 chelate-ring systems $[CuL^6]^{2+}$ possesses a relatively lower $\tilde{\nu}$ with higher intensity, indicating increased pseudo-T_d distortion induced by the C-methyl group. Such an effect would be compensated in $[CuL^7]^{2+}$ by the relative stabilization of the Cu–N bond and hence a square-based configuration, due to *N*-methylation of the benzimidazole (bzim). Compared to CuL^1, CuL^4 and CuL^3 display low ε values with no red shift, suggesting displacement of copper above the N_4 plane rather than tetrahedral distortion, as discussed above.

The complex $Cu(trien)(ClO_4)_2$ exhibits a band at 38 300 cm^{-1}, assigned to $N(\sigma)\rightarrow Cu^{II}$ charge transfer (Table 7), and so the ligand band in the range 36 000–38 000 cm^{-1} for the present complexes may have charge-transfer contributions. The band at around 26 000 cm^{-1} in the solid state and that around 29 500 cm^{-1} in solution have been assigned to $N_{het}(\pi)\rightarrow Cu^{II}$ charge transfer on the basis of their similarity to those exhibited by a Cu^{II}–bzim complex (1:8) where the $N_{het}(\pi_1)\rightarrow Cu^{II}$ and $N_{het}(\pi_2)\rightarrow Cu^{II}$ charge-transfer absorptions are resolved (Table 6); the features of the latter, in turn, are very similar to those for a copper(II) complex of 4,5-dimethylimidazole.[33] Though the positions of the ligand-field and $N_{het}\rightarrow Cu^{II}$ charge-transfer bands are similar to those for bis(benzimidazolyl)-dithioether,[8,9] the intensities of the visible band are not as enhanced as in the latter, possibly due to the unfavourable *W* term in Jorgenson's equation.[34] So we suspect that in blue proteins the intense band at 600 nm may borrow intensity mainly from $S\rightarrow Cu^{II}$ rather than from imidazolate$\rightarrow Cu^{II}$ charge-transfer absorption.

EPR Spectra.—While the polycrystalline spectra of all the CuL^1X_2 complexes are isotropic (Table 8), those of all the CuL^3 and CuL^4 complexes are axial. The frozen-solution EPR spectra of all the complexes are axial, diagnostic[32] of a $d_{x^2-y^2}$ ground state[$g_{\parallel} > g_{\perp}, g_{min} > 2.03; G = (g_{\parallel} - 2)/(g_{\perp} - 2) \approx 3.8$]. The $g_{\parallel}$ values are similar to those observed for other planar CuN_4 chromophores[29,30] and the position of the solution data on the $A_{\parallel}$ *vs.* $g_{\parallel}$ map[35] supports this. Further, the structural index[35] $g_{\parallel}/A_{\parallel}$ for all the complexes is in the range 120–135 cm, supporting a square-derived solution geometry.

On adding excess of ClO_4^- as $N(C_6H_{13})_4ClO_4$ to $CuL^1(ClO_4)_2$ in acetonitrile the cryogenic solution spectrum was resolved, suggesting that the anion may bind to copper at higher concentrations. Compared to other complexes, $CuL^1(Br)(ClO_4)$ and CuL^1Cl_2 possess higher $g_{\parallel}$ values, suggesting preferential axial interaction[31] with halide to give a square-pyramidal geometry. All these observations are consistent with the ligand-field spectral results.

The higher $g_{\parallel}$ values for CuL^4 and CuL^3 complexes, compared to CuL^1, rule out the possibility of a strictly planar stereochemistry; it is probably a more distorted square pyramid with copper(II) at the apex, as already discussed. In such a structure the orientation of the lone-pair orbital of the nitrogen donor will not be exactly along the $x^2 - y^2$ orbital of copper. So it is not unexpected that the $A_{\parallel}$ values of these compounds vary markedly in the order $CuL^3 \approx CuL^5 \approx CuL^7 > CuL^4 > CuL^6$. The lowest $A_{\parallel}$ value for CuL^6 may be due to higher tetrahedral distortion induced by the C-methyl group. Similarly, benzimidazole *N*-methylation as in CuL^2 leads to higher $A_{\parallel}$ values because of the absence of hydrogen bonding involving

---

[*] The main difference between the two structures is that in the perchlorate complex, in addition to the four equatorial nitrogens, one of the perchlorate oxygens occupies the axial position resulting in a distorted square-pyramidal co-ordination for Cu^{II}. A comparison of the two structures reveals that the present structure has been determined to a higher degree of accuracy and therefore a detailed comparison of the structural parameters is not presented. Suffice it to say that there are no gross differences in the stereochemistry of the cation in the two cases.

NH of the unsubstituted benzimidazole ring and the stronger Cu–N σ bond. Such remarkable changes in $A_{\parallel}$ values, irrespective of the change in $g_{\parallel}$, had been encountered earlier.[10] The possibility that the above significant decrease in $A_{\parallel}$ is due to increasing tetrahedral distortion from planarity cannot be discounted at this stage, in view of the observation by Sakaguchi and Addison[35] that tetrahedral distortion from planarity leads to higher $g_{\parallel}$ and lower $A_{\parallel}$ values and also the present observation that the CuL^6 complex has a higher ε value than those of the other 555 chelate-ring systems.

Aromatic nitrogen donors frequently give pronounced nitrogen hyperfine splitting in the $g_{\perp}$ region; the low or no resolution for the present compounds may be related to the loss of tetragonality in the structure,[20,31,35] as discussed above.

Electrochemical Properties.—In the cyclic voltammograms of

Table 7 Electronic absorption spectral data ($\tilde{\nu}_{max}$/cm^{-1} with ε/dm^3 mol^{-1} cm^{-1} in parentheses)

Compound	Medium	Ligand field[a]	Charge transfer[b]	Ligand[c]
$CuL^1(ClO_4)_2$	Solid	16 900	26 100	41 500 (sh)
	MeOH	15 900 (120)	29 000 (sh) (545)	36 000 (15 900) 36 900 (19 400) 40 600 (13 400)
	MeCN	16 200 (160)	29 800 (sh) (480)	35 600 (16 000) 36 900 (17 000) 40 900 (14 000)
	MeCN/$NaClO_4$	16 500 (160)		
$CuL^1(NO_3)_2$	Solid	15 300	26 100	34 600
	MeCN	15 900	28 200 (sh) (700)	36 000 (16 500) 36 900 (18 800) 39 900 (14 800)
$CuL^1(PF_6)_2·H_2O$	MeOH	16 000 (150)	28 200 (sh) (560)	36 000 (17 500) 36 900 (18 500) 40 200 (14 600)
$CuL^1Cl_2·2H_2O$	Solid	14 600	25 700	34 800
	MeOH	14 900 (101)	28 900 (sh) (304)	36 000 (27 300) 36 900 (29 000) 40 200 (19 900)
$CuL^1Br_2·2H_2O$	Solid	14 500	25 500 (sh)	34 300
	MeOH	14 900 (160)	25 900 (sh) 200)	36 000 (12 800) 36 900 (14 100) 40 800 (10 700)
$CuL^1Cl(Br)·H_2O$	Solid	14 500	25 500 (sh)	34 600
	MeOH	14 800 (125)	29 700 (sh) (150)	36 000 (12 600) 37 000 (14 600) 40 800 (2 100)
$CuL^1Br(ClO_4)·H_2O$	Solid	15 700	27 300	34 800, 36 700 40 000
	MeCN	13 400 (180)	29 600 (sh) (530)	36 000 (15 600) 37 000 (16 700) 40 900 (14 200)
$CuL^2(ClO_4)_2$	Solid	16 300	27 200 (sh)	33 000 41 400 (sh)
	MeCN	15 500 (110)	30 200 (550)	35 800 (8 800) 36 800 (10 200) 39 700 (9 300)
$CuL^3(ClO_4)_2$	Solid	16 500	30 400	34 300, 41 400
	MeOH	15 900 (60)	30 500 (sh)	35 700 (13 300) 36 500 (17 200) 40 300 (17 500)
	MeCN	16 200 (45)	31 100 (200)	35 000 (7 200) 35 900 (10 500) 36 800 (10 800) 39 200 (12 500) 39 800 (12 700)
$CuL^4(ClO_4)_2$	Solid	13 100	26 000 (sh)	33 900
	MeOH	16 200 (72)		36 200 (14 000) 37 100 (15 000) 41 300 (10 700)
$CuL^5(ClO_4)_2·H_2O$	Solid	16 900	26 600 (sh)	33 800
	MeOH	15 300 (80)	28 000 (sh) (520)	35 600 (11 000) 36 000 (14 200) 36 900 (14 100) 40 100 (16 600)
$CuL^6(ClO_4)_2$	Solid	15 900	26 100 (sh)	33 600, 40 000
	MeOH	15 900 (140)	29 900 (sh) (270)	35 800 (13 300) 36 700 (14 400) 40 300 (15 600)
	MeCN	15 900 (110)	—	35 700 (6 900) 37 000 (7 400) 41 500 (7 500)

Table 7 (*continued*)

Compound	Medium	Ligand field[a]	Charge transfer[b]	Ligand[c]
$CuL^7(ClO_4)_2{\cdot}2H_2O$	Solid	15 800	26 800 (sh)	34 500, 37 500
	MeOH	15 900 (90)	29 300 (255)	35 700 (13 300)
				36 600 (14 400)
				40 300 (15 600)
	MeCN	14 900 (45)	—	35 900 (2 350)
				36 800 (2 400)
				38 900 (2 400)
1:4 Cu^{II}–bzim	MeOH	14 700 (85)	33 100 (1 140)	35 900 (180 900)
				36 700 (210 100)
				41 200 (237 900)
1:8 Cu^{II}–bzim	MeOH	16 100 (125)	28 400 (1 540)	35 900 (29 000)
			33 100 (2 330)	36 700 (35 000)
				41 300 (39 000)
bzim ligand	MeOH	—	—	35 700 (13 900)
				36 700 (14 100)
				41 100 (15 200)
$Cu(trien)(ClO_4)_2$	MeOH	17 200 (80)	38 300 (3 770)	—

Concentrations: [a] $\approx 1 \times 10^{-2}$, [b] $\approx 1 \times 10^{-3}$ and [c] $\approx 1 \times 10^{-5}$ mol dm^{-3}. sh = Shoulder.

Table 8 Electron paramagnetic resonance spectral data[a] for the copper complexes

Compound	Medium[b]	g_0	A_0[c]	$g_\parallel$	$A_\parallel$	$g_\perp$[d]	$A_\perp$[e]
$CuL^1(ClO_4)_2$	Pc	2.058	18				
	MeOH–water	2.143	55	2.198	190	2.047	−13
$CuL^1(NO_3)_2$	Pc	2.075	18				
	MeCN	2.101	63	2.202	190	2.051	−1
$CuL^1(PF_6)_2{\cdot}H_2O$	Pc	2.056	18				
	MeOH–water	2.120	72	2.208	188	2.054	1
$CuL^1Br_2{\cdot}2H_2O$	Pc	2.059	8				
	MeOH	2.110	66	2.207	185	2.051	7
	MeOH–water	2.104	68	2.206	187	2.053	9
$CuL^1Cl_2{\cdot}2H_2O$	MeOH	2.120	70	2.230	192	2.065	9
	MeOH–$N(C_6H_{13})_4ClO_4$	—	—	2.214	178	2.063	—
$CuL^1Br(ClO_4){\cdot}H_2O$	Pc			2.195		2.065	
	MeCN–Me_2CO	2.117	63	2.222	187	2.064	1
$CuL^1Cl(Br){\cdot}H_2O$	Pc	2.062	29				
	MeOH	2.110	66	2.207	185	2.061	7
$CuL^2(ClO_4)_2$	Pc	2.059	25				
	MeOH–MeCN–Me_2CO	2.107	74	2.209	211	2.065	6
$CuL^3(ClO_4)_2$	Pc[f]	2.073	34				
	MeOH	2.112	67	2.214	189	2.059	6
$CuL^4(ClO_4)_2$	Pc			2.212		2.058	
	MeOH–Me_2CO	2.138	—	2.217	164		
$CuL^5(ClO_4)_2{\cdot}H_2O$	Pc	2.075	16				
	MeOH	2.113	61	2.214	192	2.056	−5
$CuL^6(ClO_4)_2$	Pc			2.207		2.062	
	MeOH–Me_2CO	2.101	80	2.217	135	2.079	53
$CuL^7(ClO_4)_2{\cdot}2H_2O$	Pc			2.234		2.077	
	MeOH–Me_2CO	2.113	67	2.229	189	2.053	6

[a] Values determined as described in the Experimental section; $A_\parallel$ values in 1×10^{-4} cm^{-1}. [b] Pc = Polycrystalline. Methanol–acetone (4:1 v/v) and acetonitrile–methanol–acetone (2:1:1). [c] One-third of the width between the first-derivative spectrum's maximum and minimum. [d] $g_\perp = \frac{1}{2}(3g_0 - g_\parallel)$. [e] $A_\perp = \frac{1}{2}(3A_0 - A_\parallel)$. [f] Very broad axial feature.

all the complexes one reduction wave occurs in the potential range −0.45 to −0.61 V (Table 9), with a directly associated oxidation wave in the reverse scan (Fig. 2). An additional anodic wave is discernible in most cases. For CuL^1Cl_2 in MeOH there is one nearly quasi-reversible wave I (Fig. 3) corresponding to $[CuL^1]^{2+}$ species (Table 9) and an irreversible wave II probably due to $[CuL^1(Cl)]^+$ species. A third wave (III) may correspond to $[CuL^1Cl_2]$. With increase in scan rate peak I grows at the expense of II and on the incremental addition of Cl^- as NBu_4Cl wave II grew at the expense of I; this lends support to the existence of the equilibrium $[CuL^1(Cl)]^+ \rightleftharpoons [CuL^1]^{2+} + Cl^-$. A similar behaviour was observed for the dibromide.

The diffusion coefficients (D) of the complexes were calculated from the cyclic voltammograms by plotting i_{pc} *vs.* $v^{\frac{1}{2}}$ for scan rates of 0.01–0.2 V s^{-1} and substituting the slope obtained in the Randler–Sevcik equation.[36] The Dη values [$(1.2\text{–}3.6) \times 10^{-8}$ g cm s^{-2}] are typical of $n = 1$ rather than $n = 2$ processes[35,37] (where n is the number of electrons transferred) and are similar to those obtained for analogous systems.[28]

All the copper complexes exhibit quasi-reversible to irreversible Cu^{II}–Cu^I redox behaviour, as evident from the observed ΔE_p and i_{pa}/i_{pc} values (Table 9) (59 mV and 1 respectively for a Nernstian one-electron redox system). The i_{pa}/i_{pc} value for $CuL^1(ClO_4)_2$ is constant (≈ 0.95) in acetonitrile but in MeOH decreases with scan rate, indicating probable dissociation of co-ordinated anion in acetonitrile. The non-Nernstian behaviour may be ascribed to heterogeneous electron-transfer kinetics and a coupled chemical reaction. The latter is evident from the cathodic shift of the reduction peak and the anodic shift of

Table 9 Electrochemical data[a] for the CuN_4 systems at 25 °C

Complex	Solvent	E_{pc}/V	E_{pa}/V	$E_{\frac{1}{2}}$/V	ΔE_p/mV	$\Delta E_p{}^0$ [b]/mV	i_{pa}/i_{pc}	$E_{\frac{1}{2}}$ [c]/V	$10^6 D$/$cm^2\ s^{-1}$	$10^8 D\eta$ [d]/g cm s^{-2}
$CuL^1(ClO_4)_2$	MeOH	−0.560	−0.456	−0.508	104	70	0.89	−0.505	3.10	2.0
	MeOH–ClO_4^-	−0.586	−0.488	−0.537	98		1.09	—		
	MeCN	−0.596	−0.486	−0.541	110	80	0.87	−0.543	3.60	2.3
$CuL^1Cl_2\cdot 2H_2O$	MeOH	−0.552	−0.460	−0.506	92	—	—	−0.517	—	—
		−0.408	[e]	—	—	—	—	−0.365	—	—
		0.142	0.310	0.226	168			0.137		
$CuL^1Br_2\cdot 2H_2O$	MeOH	−0.570	−0.488	−0.529	82	—	—	−0.526	—	—
		−0.372	[e]	−0.288	—	—	—	[f]	—	—
		0.124	0.262	0.193	138			[f]		
$CuL^2(ClO_4)_2$	MeCN	−0.608	−0.512	−0.560	96	101	0.97	−0.562	1.77	1.2
$CuL^3(ClO_4)_2$	MeOH	−0.530	—	—	—	—	—	−0.458	—	—
		—	0.200[g]					0.148		
$CuL^4(ClO_4)_2$	MeOH	−0.476	−0.320	−0.398	156	—	1.17	−0.405	4.1	2.7
		—	0.194[g]					0.129		
$CuL^5(ClO_4)_2\cdot H_2O$	MeOH	−0.518	−0.360	−0.439	158	—	1.58	−0.431	2.69	1.7
		—	0.146[g]							
$CuL^6(ClO_4)_2$	MeOH	−0.466	−0.332	−0.399	134	124	0.86	—	5.52	3.6
		—	0.188[g]				1.89			
$CuL^7(ClO_4)_2\cdot 2H_2O$	MeOH	−0.505	−0.338	−0.422	167	—	0.85	−0.397	2.10	1.3
		—	0.174[g]							

[a] Measured *vs.* non-aqueous silver reference electrode; add 0.544 V to convert into NHE. Scan rate 50 mV s^{-1}. Supporting electrolyte tetra-*n*-hexylammonium perchlorate (0.1 mol dm^{-3}). Concentration 1 mmol dm^{-3} in complex. [b] $\Delta E_p{}^0$ is ΔE_p at zero i_{pc}. [c] Differential Pulse Voltammetry (DPV), scan rate 1 mV s^{-1}, pulse height 50 mV. [d] η value, 0.00651 g cm^{-1} s^{-1} from ref. 9. [e] Difficult to detect. [f] DPV not carried out. [g] Additional anodic peak.

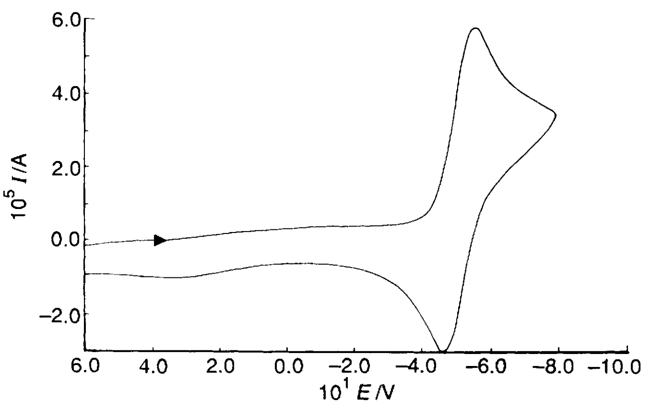

Fig. 2 Cyclic voltammograms of 1 mmol dm^{-3} $CuL^1(ClO_4)_2$ in methanol at 25 °C. Supporting electrolyte: 0.1 mol dm^{-3} $N(C_6H_{13})_4$-ClO_4. Scan rate 0.05 V s^{-1}

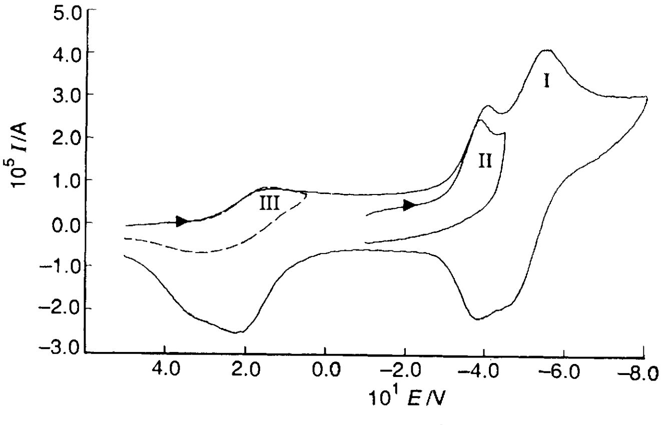

Fig. 3 Cyclic voltammograms of 1 mmol dm^{-3} CuL^1Cl_2 in MeOH at 25 °C. Details as in Fig. 2

the oxidation wave with increase in scan rate.[36] Based on $\Delta E_p{}^0$ (Table 8), the decreasing order of reversibility is CuL^1 > CuL^2 > CuL^6 and that based on the ΔE_p at 50 mV s^{-1} scan rate is CuL^1 > CuL^6 > CuL^4 ≈ CuL^5 > CuL^7. It is difficult to draw quantitative conclusions on the structural rearrangements accompanying electron transfers based only on ΔE_p; however, the above orders illustrate that the bulky benzimidazoles, the flexible six-membered chelate ring and steric crowding by the CMe group tend to confer reversibility.

All the complexes exhibit relatively positive Cu^{II}–Cu^{I} redox potentials (*vs.* normal hydrogen electrode, NHE) in the order CuL^1 < CuL^3 < CuL^4, indicating that the 656 and 565 rather than 555 or 666 chelate rings are ideally suited to establish strong in-plane σ interactions with copper(II). A similar dependence of $E_{\frac{1}{2}}$, *viz.* 656 < 565 < 555 < 666 for related copper(II) tetraamine[38] complexes, but interestingly a reverse order, *viz.* 656 > 565 > 555, for bis(pyridyl)diaza complexes,[39] have been observed. Thus, while the higher bites of six-membered chelate rings are suitable for stronger in-plane Cu^{II}–N σ interaction, their six-membered chelate ring flexibility is suitable for efficient Cu–N π interaction and favours a pseudo-T_d co-ordination geometry for Cu^I.

Further, the tetraamine complexes exhibit variation in $\tilde{\nu}$(d–d) depending on chelate-ring size; this shows that not only tetrahedral distortion[40] from planarity or trigonal-bipyramidal geometry but also displacement of copper above the square plane with weak Cu–N bonds, as in [Cu(trien)(SCN)]SCN[28] with a 555 chelate-ring system, would result in a decrease in $\tilde{\nu}$(d–d) (16 800–18 900 cm^{-1})[29] (and in turn crystal-field stabilization energy[40]) and hence ΔH_{eq} and $E_{\frac{1}{2}}$, in the order, 656 ≈ 565 < 555 < 666. However, within pyridine and benzimidazole complexes, the variation in the chelate-ring size does not affect $\tilde{\nu}$(d–d) significantly, but does the $E_{\frac{1}{2}}$ values. The decrease in $\tilde{\nu}$(d–d) for all these copper(II) complexes[29,39] in the order ($E_{\frac{1}{2}}$/V values in parentheses), 16 800–18 900 (−0.50 to −0.28[38]) (amine) > 16 550 (−0.19 to −0.13) (pyridine[39]) > 16 000 (−0.02 to +0.11) (benzimidazole) represents a decrease in the in-plane Cu–N σ interaction due to increase in tetrahedral distortion and/or displacement of copper above the N_4 plane, induced by the increasingly bulky donors and illustrates the above variation in $E_{\frac{1}{2}}$. The higher $E_{\frac{1}{2}}$ values[39] for the pyridine and benzimidazole complexes would also be due in part to the π-accepting ability[40] of the heterocyclic rings. Thus the presence of four pyridyl nitrogens as in $CuL^9(ClO_4)_2$ results[27] in an $E_{\frac{1}{2}}$ enhancement, compared to the corresponding bis(pyridine) complex.[39]

Conclusion

The present study leads to the conclusion that when copper(II)–ligand σ interactions dominate as in complexes of a number of open-chain bis(benzimidazolyl)diaza ligands, the replacement of a six- by a five-membered chelate ring leads to further displacment of copper from the tetrahedrally distorted co-ordination plane and elevates $E_{\frac{1}{2}}$. On the other hand, when π interactions and steric constraints are important such a replacement would tend to confer a trigonal-bipyramidal configuration around copper(II) and hence a higher $E_{\frac{1}{2}}$. This conclusion is supported by the $E_{\frac{1}{2}}$ variation in complexes with CuN_2S_2 chromophores derived from bis(pyridyl)dithia[39] and bis(benzimidazolyl)dithia[9] ligands, where π interactions are important. Also in copper complexes of macrocyclic ligands[41] and open-chain tetrathioether dicarboxylic acids,[42] both with CuS_4 chromophores, and in corresponding complexes[42] of bis(benzimidazolyl)tetrathia ligands, with CuN_2S_4 chromophores, the same situation prevails. Further, the copper complexes of bis(benzimidazolyl)dithia ligands[9] behave similarly to those of open-chain diazadithia ligands,[41,43] indicating that thioether is not as good a π acceptor as is pyridine.

The present investigation suggests that an increase in steric hindrance as well as π interaction, irrespective of the chelate-ring sizes, may favour a pseudo-T_d geometry suitable for Cu^I and raise $E_{\frac{1}{2}}$. This is possibly the situation in blue copper proteins where the π-back bonding ability of sulfur and the approximately tetrahedral co-ordination enforced around copper by the very large chelate-ring sizes in the superstructure account for the high redox potentials.

Thioether rather than imidazole co-ordination in blue proteins may be mainly responsible for their intense charge-transfer absorption.

Acknowledgements

We are grateful to the Department of Science and Technology (Grant No. SP/S1/IO4/86), New Delhi, India, for the generous support of this work. The C, H and N analyses were performed at City University, London by Professor S. A. Matlin, thanks to the support of the International Organization for Chemical Sciences in Development (IOCD). Dr. T. K. Chandrasekar, Indian Institute of Technology, Kanpur, is thanked for recording some EPR spectra.

References

1 P. M. Colman, H. C. Freeman, J. M. Guss, M. Murata, V. A. Norris, J. A. M. Ramshaw and M. P. Venkatappa, *Nature (London)*, 1978, **272**, 319; J. M. Guss and H. C. Freeman, *J. Mol. Biol.*, 1983, **169**, 521.

2 E. T. Adamn, R. E. Stenkamp, L. C. Sieker and L. H. Jensen, *J. Mol. Biol.*, 1978, **125**, 35; G. E. Norris, B. F. Anderson and E. N. Baker, *J. Am. Chem. Soc.*, 1986, **108**, 2784.

3 D. E. Wilcox, J. R. Long and E. I. Solomon, *J. Am. Chem. Soc.*, 1984, **106**, 2186.

4 A. C. van Steenbergen, E. Bouwman, R. A. G. de Graaff, W. L. Driessen and J. Reedijk, *J. Chem. Soc., Dalton Trans.*, 1990, 3175.

5 K. J. Oberhausen, R. J. O'Brien, J. F. Richardson and R. M. Buchanan, *Inorg. Chim. Acta*, 1990, **173**, 145; K. J. Oberhausen, W. D. Easley, J. F. Richardson and R. M. Buchanan, *Acta Crystallogr., Sect. C*, **47**, 2037.

6 J. van Rijn, W. L. Driessen, J. Reedijk and J. M. Lehn, *Inorg. Chem.*, 1984, **23**, 3584.

7 P. J. M. W. L. Birker, J. Helder, G. Henkel, B. Krebs and J. Reedijk, *Inorg. Chem.*, 1982, **21**, 357.

8 A. W. Addison, T. Nageswara Rao, J. Reedijk, J. van Rijn and G. C. Verschoor, *J. Chem. Soc., Dalton Trans.*, 1984, 1349.

9 A. W. Addison, M. Palaniandavar, T. N. Rao, J. Reedijk and J. van Rijn, unpublished work.

10 Y. Nishida and K. Takahashi, *J. Chem. Soc., Dalton Trans.*, 1988, 691.

11 T. Pandiyan, M. Palaniandavar, M. Lakshminarayanan and H. Manohar, unpublished work.

12 S. Usha, T. Pandiyan and M. Palaniandavar, *Indian J. Chem., Sect B*, in the press.

13 D. J. E. Ingram, in *Spectroscopy at Radio and Microwave Frequencies*, Butterworths, London, 1955, p. 305; D. Kosman and R. Bereman, in *Spectroscopy in Biochemistry*, ed. J. E. Bell, CRC Press, Boca Raton, FL, 1981, vol. 2.

14 A. T. C. North, C. C. Phillips and F. S. Mathews, *Acta Crystallogr. Sect. A*, 1968, **24**, 351.

15 G. M. Sheldrick, SHELX 76, a Program for Crystal Structure Determination, University of Cambridge, 1976.

16 C. K. Johnson, ORTEP II, a Program for Thermal Ellipsoid Plotting, Oak Ridge National Laboratory, Oak Ridge, TN, 1976.

17 S. Motherwell and W. Clegg, PLUTO, a Program for Drawing Crystal and Molecular Structures, University of Cambridge, 1978.

18 *International Tables for X-Ray Crystallography*, Kynoch Press, Birmingham, 1974, vol. 4.

19 D. K. Towle, S. K. Hoffman, W. E. Hatfield, P. Chaudhuri and K. Wieghardt, *Inorg. Chem.*, 1985, **24**, 4393.

20 A. W. Addison, P. J. Burke, K. Jenrick, T. Nageswara Rao and E. Sinn, *Inorg. Chem.*, 1983, **22**, 3645.

21 P. J. W. M. L. Birker, E. F. Godefroi, J. Helder and J. Reedijk, *J. Am. Chem. Soc.*, 1982, **104**, 7556.

22 W. L. Duax, C. M. Weeks and D. C. Rohrer, *Top. Stereochem.*, 1976, **9**, 279.

23 S. Juen and Z. Yishen, *Inorg. Chim. Acta*, 1989, **162**, 29.

24 P. Nagle, E. O'Sullivan and B. J. Hathaway, *J. Chem. Soc., Dalton Trans.*, 1990, 3399.

25 A. W. Addison, in *Copper Coordination Chemistry: Biochemical and Inorganic Perspectives*, eds. K. D. Karlin and J. A. Zubieta, Adenine Press, Guilderland, NY, 1983, p. 109.

26 G. Marongiu, E. C. Lingafelter and P. Paoletti, *Inorg. Chem.*, 1969, **8**, 2763.

27 T. Garber, S. V. Wallendael, D. P. Rillema, M. Kirk, W. E. Hatfield, J. H. Welch and P. Singh, *Inorg. Chem.*, 1990, **29**, 2863.

28 A. W. Addison, M. Palaniandavar, W. L. Driessen, F. Paap and J. Reedijk, *Inorg. Chim. Acta*, 1988, **142**, 95.

29 L. Fabbrizzi, P. Paoletti and A. B. P. Lever, *Inorg. Chem.*, 1976, **15**, 1502.

30 A. W. Addison, M. Carpenter, L. K. M. Lau and M. Wicholas, *Inorg. Chem.*, 1978, **17**, 1545.

31 Y. Nonaka, T. Toku and S. Kida, *Bull. Chem. Soc. Jpn.*, 1974, **47**, 312.

32 B. J. Hathaway and D. E. Billing, *Coord. Chem. Rev.*, 1970, **5**, 143.

33 H. J. Schugar, in *Copper Coordination Chemistry: Biochemical and Inorganic Perspectives*, eds. K. D. Karlin and J. A. Zubieta, Adenine Press, Guilderland, NY, 1983, p. 49.

34 C. K. Jorgensen, in *Oxidation Numbers and Oxidation States*, Springer, New York, 1969, p. 144.

35 U. Sakaguchi and A. W. Addison, *J. Chem. Soc., Dalton Trans.*, 1979, 600.

36 A. J. Bard and L. R. Faulkner, in *Electrochemical Methods: Fundamental Applications*, Wiley, New York, 1980, p. 218.

37 A. W. Addison, T. N. Rao and E. Sinn, *Inorg. Chem.*, 1984, **23**, 1957.

38 L. Fabbrizzi, A. Poggi and P. Zanello, *J. Chem. Soc., Dalton Trans.*, 1984, 1495.

39 D. E. Nikles, M. J. Powers and F. L. Urbach, *Inorg. Chem.*, 1983, **22**, 3210.

40 H. Yokoi and A. W. Addison, *Inorg. Chem.*, 1977, **16**, 1341.

41 E. R. Dockal, T. E. Jones, E. E. Sokol, R. J. Engerer, D. B. Rorabacher and L. E. Ochrymowycz, *J. Am. Chem. Soc.*, 1976, **98**, 4322.

42 S. Usha and M. Palaniandavar, unpublished work.

43 T. A. Kaden, S. Kaderli, W. Sagar, L. C. Siegfried-Hertli and A. Zuberbuhler, *Helv. Chim. Acta*, 1986, **69**, 1217.

Received 28*th April* 1992; *Paper* 2/02192G